Polarization Observables in Elastic Electron-Deuteron Scattering[*]

E. M. Darwish[1,2,3], M. Y. Hussein[4], and B. Abu Sal[5]

[1]Department of Applied Physics, Faculty of Applied Sciences, Taibah University
P. O. Box 1343, Al-Madinah Al-Munawarah, Kingdom of Saudi Arabia

[2]Physics Department, Faculty of Science, Sohag University, Sohag 82524, Egypt

[3]Egyptian Center for Theoretical Physics, MTI, Al-Mukattam, Cairo, Egypt
Email Address: eeddarwish@yahoo.com

[4]Physics Department, College of Science, Bahrain University
P. O. Box 32038, Kingdom of Bahrain

[5]Department of Applied Physics, Faculty of Applied Sciences, Taibah University
P. O. Box 1343, Al-Madinah Al-Munawarah, Kingdom of Saudi Arabia

Polarization oberables in elastic electron-deuteron scattering are predicted and compared with recent experimental data. Particular attention is paid to the tensor-deuteron analyzing power T_{20} and the beam-vector-deuteron analyzing power T_{11}^e because of their importance in extracting the deuteron electromagnetic form factors which provide an intuitive picture of the internal deuteron structure. This study is made possible with the advent of recent polarization measurements at JLab and MIT-Bates with polarized electron beam and polarized deuteron target. The sensitivity of the results to deuteron wave functions of different high-precision NN potentials is investigated. We found that the analyzing powers, predicted using different NN potentials, agree with one another and with experimental data. The T_{20} asymmetry is found to be slightly dependent on the electron scattering angle up to $\theta_e \simeq 120°$, whereas the analyzing power T_{11}^e is found to be sensitive to the electron angle.

Keywords: Spin observables, elastic electron scattering, deuteron, electromagnetic form factors, nucleon-nucleon interactions.

1 Introduction

With the advent of high-intensity and high-duty-cycle electron accelerators, experiments with beam energies of several GeV and high momentum transfers have become feasible and are carried out at several laboratories around the world, such as the Thomas Jefferson National Accelerator Facility (JLab) in Newport News, VA (USA), MIT-Bates

---

[*]Presented by the first author at the 4th Annual Meeting of the Saudi Physical Society held at the King Abdulaziz City for Science and Technology, Riyadh, Saudi Arabia, November 11-12, 2008.

in Middleton, MA (USA), and MAMI in Mainz (Germany). For up-to-date information on these experiments and their theoretical interpretation, we refer the reader to the recent reviews [1–3]. In particular, electron scattering beams are used at MIT-Bates for medium energy electron scattering studies in which the electromagnetic properties of the nucleons and nucleus are probed by exchange of virtual photons between the probing electron and the target. Energy and momentum transfer can vary independently, in contrast to the case of real photoabsorption. For this reason electron scattering constitutes a much richer field to study the dynamics of a nuclear system. With the development of the new facilities, and thanks to improvements in polarized beam and polarized target techniques, as well as recoil polarization measurements, it is now possible to obtain accurate data for electron scattering, including spin-dependent observables.

The study of polarization observables in electroweak reactions is an important tool in order to investigate small but interesting dynamical effects, which normally are buried under the dominant amplitudes in unpolarized total and differential cross sections, but which often may show up significantly in certain polarization observables. The reason for this feature lies in the fact that such small amplitudes or small contributions to large amplitudes may be amplified by interference with dominant amplitudes, or that dominant amplitudes interfere destructively leaving thus more room to the small amplitudes [4]. For example, this fact has been exploited in elastic electron-deuteron scattering in order to disentangle the charge quadrupole form factor G_Q from the monopole one G_C by measuring the tensor-deuteron analyzing power T_{20} or equivalently the tensor-deuteron recoil polarization P_{20}. The tensor-deuteron analyzing power T_{20} is the dominant observable in separating the deuteron electromagnetic form factors and is the subject of many experimental and theoretical works (see [1–3] and references therein). The deuteron tensor polarization has also been considered as an important tool for probing the nucleon-nucleon (NN) interaction at short distances [5, 6], making it possible to choose among different model deuteron wave functions, that is, among different models of the NN interaction.

Alternatively, one may deal with beam-vector-deuteron double polarization only if the electron beam is also polarized. This type of experiment has been performed most recently at MIT-Bates by using both a polarized electron beam and a polarized target [7, 8]. The beam-vector-deuteron analyzing power T_{11}^e has been measured in the region of low momentum transfer [7]. This means that in addition to the tensor-deuteron analyzing power T_{20}, one has access to the beam-vector-deuteron double polarization observable T_{11}^e of a longitudinally polarized electron beam and a polarized deuteron target. The T_{11}^e asymmetry turns out to be dominated by the interference of the electric monopole and magnetic dipole form factors at low momentum transfer. Since the former is known to within a few percent in this region [9], one can use a measurement of T_{11}^e to extract information on the magnetic dipole form factor.

The main goal of the present paper is, therefore, to investigate the elastic electron-

deuteron scattering process with special emphasize on the tensor- and the beam-vector-deuteron analyzing powers T_{20} and T_{11}^e, respectively. Their sensitivity to the most popular deuteron wave functions obtained from modern high-precision NN interactions will be studied. In addition, we compare our predictions for the T_{20} and T_{11}^e asymmetries, based on various NN interaction models, with the existing experimental data [7, 10–16]. This investigation will be a crucial step in understanding the internal electromagnetic structure of the deuteron.

The article is organized as follows. In Sec. 2, the basic ingredients for elastic electron-deuteron scattering are briefly reviewed. The general definition of the unpolarized and the polarized cross sections, as well as the relevant expressions for the tensor- and beam-vector-deuteron analyzing powers T_{20} and T_{11}^e, respectively, are given. Sec. 3 contains the results on the analyzing powers T_{20} and T_{11}^e. In the same section we also compare our predictions with data available in the considered kinematic region. Sec. 4 presents the conclusion.

2 Elastic Electron-Deuteron Scattering Including Analyzing Powers

From quantum electrodynamics, the differential cross section for the elastic scattering of unpolarized electrons of initial (final) energy E (E') from an unpolarized deuteron target with internal structure can be written in the Born approximation of a one-photon-exchange mechanism, neglecting the electron mass, as [17]

$$\frac{d\sigma_0}{d\Omega_e} = \left(\frac{d\sigma}{d\Omega}\right)_{Mott} \frac{E'}{E} \left[A(Q^2) + B(Q^2)\tan^2\frac{\theta_e}{2}\right], \qquad (2.1)$$

where θ_e is the electron scattering angle in the laboratory frame, $Q^2 = 4EE'\sin^2(\theta_e/2)$ is the squared four-momentum transfer, and $(d\sigma/d\Omega)_{Mott}$ is the Mott cross-section.

The unpolarized elastic structure functions $A(Q^2)$ and $B(Q^2)$ allow us to create a phenomenological description of the underlying structure of the deuteron. These structure functions can be written in terms of the deuteron elastic form factors as [2]

$$A(Q^2) = G_C^2 + \frac{8}{9}\tau^2 G_Q^2 + \frac{2}{3}\tau G_M^2, \qquad (2.2)$$

$$B(Q^2) = \frac{4}{3}\tau(1+\tau)G_M^2, \qquad (2.3)$$

where $\tau = Q^2/(4M_D^2)$, M_D denotes the deuteron mass. In unpolarized elastic electron-deuteron scattering experiments, the structure functions $A(Q^2)$ and $B(Q^2)$ can only be measured by determining $B(Q^2)$ directly from the backward scattering cross-section. Equation (2.3) yields the magnetic form factor G_M, but the charge monopole G_C and the charge quadrupole G_Q form factors cannot be separated in Eq. (2.2). Therefore, one needs an additional third observable to get information on all three deuteron form factors separately. The third observable of choice is the dependence of the scattering on the deuteron polarization.

The differential cross-section for elastic scattering of a longitudinally polarized electron beam from a polarized deuteron target is given in the laboratory frame by [18]

$$\frac{d\sigma}{d\Omega_e}(h, P_z, P_{zz}) = \Sigma(\theta^*, \phi^*) + h\Delta(\theta^*, \phi^*),\tag{2.4}$$

where $h = \pm 1/2$ is the helicity of the incident electron beam; that is the projection of the electron spin in the direction of its three-momentum. P_z and P_{zz} are the degree of vector and tensor polarization of the deuteron target. The polarization direction of the deuteron is defined by the angles θ^* and ϕ^* in the frame where the z-axis is along the direction of the virtual photon and the y-axis is defined by the vector product of the incoming and the outgoing electron momenta. This is illustrated in Fig. 2.1.
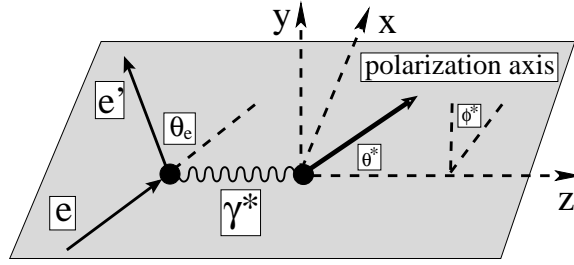

Figure 2.1: Conventions of the scattering plane.

The first term on the right-hand side in Eq. (2.4) gives the cross section for an unpolarized electron but a polarized target deuteron and contains the tensor-deuteron analyzing powers T_{20}, T_{21}, and T_{22}, which may be written as

$$\Sigma(\theta^*, \phi^*) = \frac{d\sigma_0}{d\Omega_e}\left[1 + \Gamma(\theta^*, \phi^*)\right],\tag{2.5}$$

where $d\sigma_0/d\Omega_e$ denotes the unpolarized differential cross-section given in Eq. (2.1) and $\Gamma(\theta^*, \phi^*)$ is given by

$$\Gamma(\theta^*, \phi^*) = P_{zz}\left[\frac{1}{\sqrt{2}}\, P_2^0(\cos\theta^*)\, T_{20}(Q^2, \theta_e) - \frac{1}{\sqrt{3}}\, P_2^1(\cos\theta^*)\, \cos\phi^*\, T_{21}(Q^2, \theta_e)\right.$$
$$\left. + \frac{1}{2\sqrt{3}}\, P_2^2(\cos\theta^*)\, \cos 2\phi^*\, T_{22}(Q^2, \theta_e)\right].\tag{2.6}$$

The second term on the right-hand side in Eq. (2.4) gives the helicity-dependent differential cross-section for a polarized electron beam and a polarized deuteron target and contains the beam-vector-deuteron analyzing powers T_{10}^e and T_{11}^e, and is given by

$$h\Delta(\theta^*, \phi^*) = \frac{d\sigma_0}{d\Omega}hP_z\left[\frac{\sqrt{3}}{2}P_1(\cos\theta^*)\, T_{10}^e(Q^2, \theta_e) - \sqrt{3}P_1^1(\cos\theta^*)\, \cos\phi^*\, T_{11}^e(Q^2, \theta_e)\right],\tag{2.7}$$

where the Legendre polynomials $P_\ell(x)$ and the associated Legendre polynomials $P_\ell^m(x)$ are taken according to the Edmonds convention [19].

With respect to polarization observables, we focus in this paper only on the tensor-deuteron T_{20} and the beam-vector-deuteron T_{11}^e analyzing powers. Following the Madison convention [20], these analyzing powers are defined as [2,21,22]

$$T_{20}(Q^2, \theta_e) = -\sqrt{2}\frac{\tau}{S}\left(\frac{4}{3}G_C G_Q + \frac{4}{9}\tau G_Q^2 + \frac{1}{6}\left[1 + 2(\tau+1)\tan^2\left(\frac{\theta_e}{2}\right)\right]G_M^2\right), \quad (2.8)$$

$$T_{11}^e(Q^2, \theta_e) = \frac{2}{\sqrt{3}}\frac{1}{S}\sqrt{\tau(1+\tau)}\,G_M\left[G_C + \frac{\tau}{3}G_Q\right]\tan\left(\frac{\theta_e}{2}\right), \quad (2.9)$$

where $S = A(Q^2) + B(Q^2)\tan^2(\theta_e/2)$. Definition of other analyzing powers are given in [22], to which the reader is referred for more details.

3 Results and Discussion

In this section, we present and discuss our results for the tensor-deuteron analyzing power T_{20} and the beam-vector-deuteron analyzing power T_{11}^e. Their sensitivity to the deuteron wave functions of various modern NN potentials is investigated. Furthermore, we compare our results for the analyzing powers with the existing experimental data.

The ingredients for the present calculation are the deuteron wave functions of the various NN potentials and the free nucleon form factors. The calculation was made with the use of the free-nucleon form factors obtained in [23]. For the deuteron wave functions, we consider five high-precision NN interactions. These are the Paris [24], the Argonne $v18$ [25], the Nijmegen (Nijm-93) [26], the one solitary boson-exchange (OSBEP) [27], and the CD-Bonn [28] potential models.

3.1 The tensor-deuteron analyzing power T_{20}

We start the discussion by presenting the results for the tensor-deuteron analyzing power T_{20} as shown in Figs. 3.2 and 3.3. In Fig. 3.2 we present the asymmetry T_{20} as a function of the squared four-momentum transfer Q^2 calculated at various electron scattering angles θ_e in the laboratory frame, whereas in Fig. 3.3 the results of T_{20} are shown as a function of Q^2 at a fixed value of electron scattering angle $\theta_e = 70°$. In order to examine the predictions of the various models for the NN interaction, we compare the results of T_{20} with the available experimental data as shown in Fig. 3.3. We found that the T_{20} asymmetry is nearly independent of the free nucleon form factors and, in particular, of the poorly known neutron electric form factor. It is also found that, the analyzing power T_{20} is slightly dependent on the electron scattering angle up to $\theta_e \simeq 120°$ since its values are nearly the same in this region. This follows from Eqs. (2.3) and (2.8), because T_{20} goes
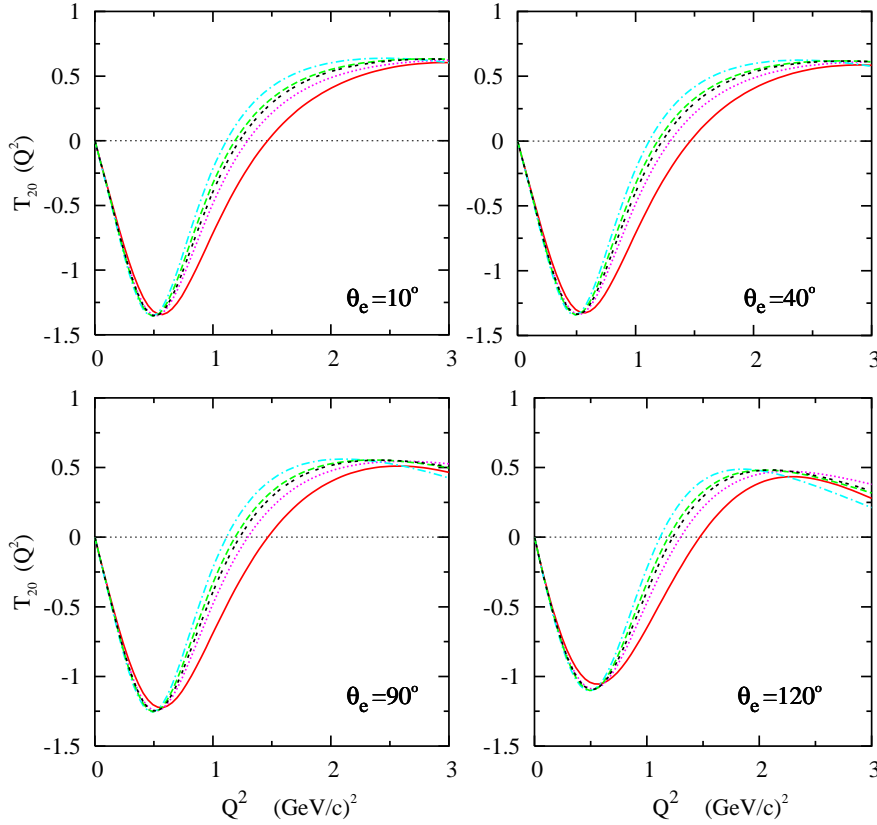
Figure 3.2: (Color online) The tensor-deuteron analyzing power T_{20} as a function of the squared four-momentum transfer Q^2 calculated at various electron scattering angles θ_e in the laboratory frame for a variety of phenomenological modern NN potentials and the nucleon form factors from [23]. Curve conventions: solid, results using the CD-Bonn potential [28]; dotted, Nijm-93 [26]; double-short-dashed, OSBEP [27]; long-dashed, AV18 [25]; dash-dotted, Paris [24].

to the constant limit $-1/(2\sqrt{2})$ at backward electron scattering angles. This means that at extreme backward angles the form of curves in Fig. 3.2 have to be changed drastically.

Fig. 3.3 shows that none of the NN potentials used could reproduce the world data of T_{20} for a squared four-momentum transfer $Q^2 > 0.75$ (GeV/c)^2. In this range of momentum transfer, the theoretical description of the polarization tensor T_{20} depends on the choice of the form of the NN interaction. On the other hand, one sees that the potential models used are consistent with the T_{20} data in the low-Q^2 region, given that they hardly differ among themselves and the data have fairly large discrepancies.
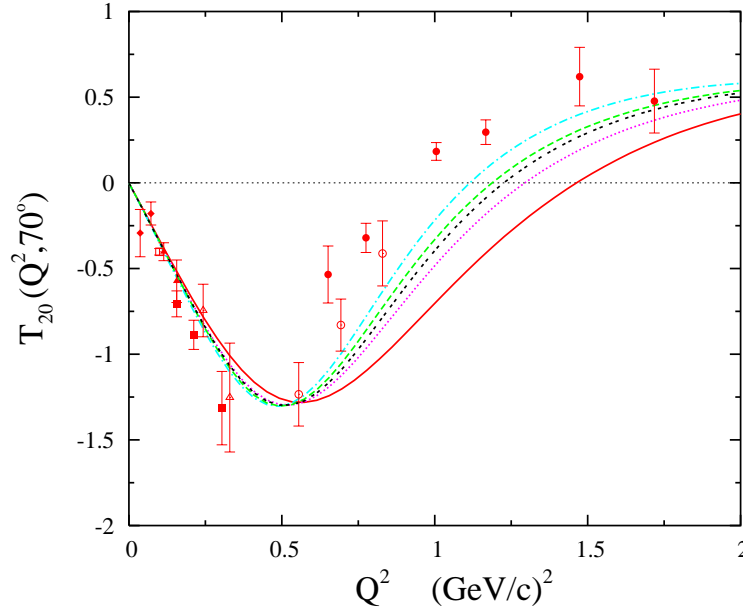
Figure 3.3: (Color online) The tensor-deuteron analyzing power T_{20} as a function of Q^2 calculated at $\theta_e = 70°$ for a variety of NN potentials and the nucleon form factors from [23]. Curve conventions as in Fig. 3.2. Experimental data are from MIT-Bates [10] (solid triangles), Novosibirsk VEPP-2 [11] (solid diamonds), Novosibirsk VEPP-3 [12] (open triangles), MIT-Bates [13] (open circles), NIKHEF [14] (open squares), NIKHEF [15] (solid squares), and JLab [16] (solid circles).

3.2   The beam-vector-deuteron analyzing power T_{11}^e

Next, we discuss the results for the beam-vector-deuteron analyzing power T_{11}^e as shown in Figs. 3.4, 3.5, and 3.6. In Fig. 3.4 we present the T_{11}^e asymmetry as a function of the squared four-momentum transfer Q^2 calculated at various electron scattering angles θ_e in the laboratory frame, whereas in Fig. 3.5 we show the results of T_{11}^e as a function of the electron scattering angle θ_e in the laboratory frame predicted at $Q^2 = 1.0$ (GeV/c)^2 and 1.4 (GeV/c)^2 with different NN potential models. Fig. 3.6 shows a comparison between our results for the T_{11}^e asymmetry and the existing experimental data.

In contrast to the case of the analyzing power T_{20}, we found that the beam-vector-deuteron double polarization asymmetry T_{11}^e is sensitive to the electron scattering angle θ_e in the laboratory frame (see Fig. 3.4). In order to show the sensitivity of the analyzing power T_{11}^e to the electron scattering angle, we illustrate in Fig. 3.5 this polarization observable versus θ_e at two different values of the squared four-momentum transfer $Q^2 = 1.0$ (GeV/c)^2 (left panel) and 1.4 (GeV/c)^2 (right panel) for the five NN potential models used. It is clear that each potential has its own peak value. It is found that, for the five NN
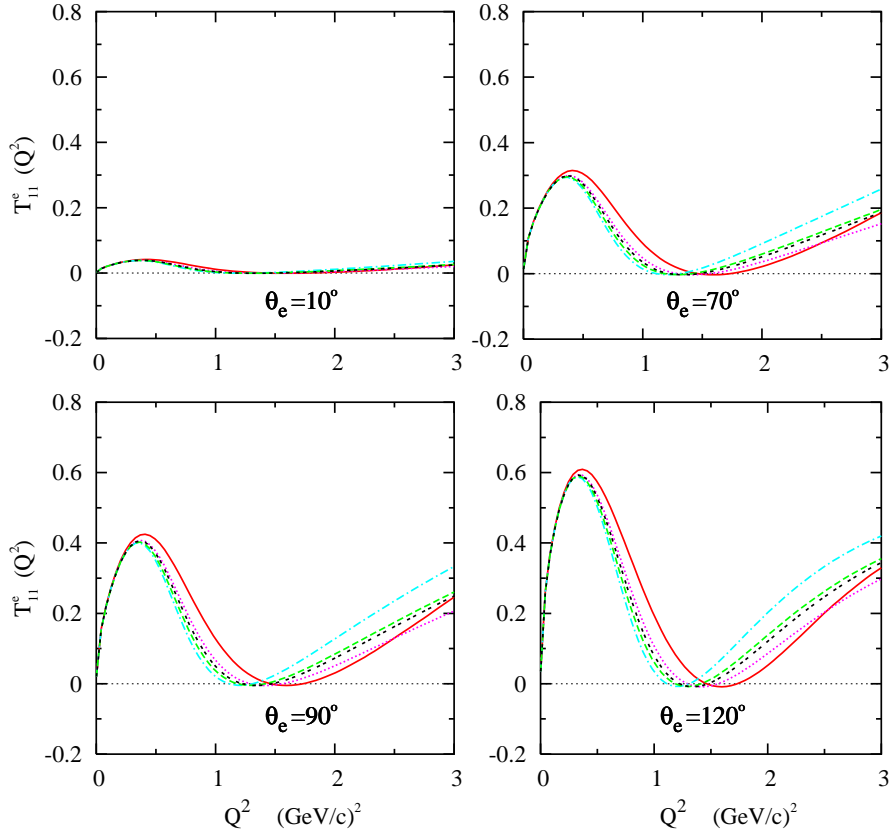
Figure 3.4: (Color online) The beam-vector-deuteron analyzing power T_{11}^e as a function of Q^2 predicted at various electron scattering angles θ_e in the laboratory frame with different NN potentials. Curve conventions are as in Fig. 3.2.

potential models, the analyzing power T_{11}^e can distinguish between competing models at backward angle and a peak is found for each potential model at $\theta_e \simeq 150°$.

Most recently, the beam-vector-deuteron double polarization asymmetry T_{11}^e has been measured using the BLAST detector at MIT-Bates [7]. This experiment covers a range of four-momentum transfer $Q < 2.5$ fm^{-1}, that shows little potential model dependence. This can be seen in the plots of the T_{11}^e asymmetry shown in Fig. 3.6 as a function of Q^2 at a fixed value of $\theta_e = 40°$. As has been remarked above in the case of tensor-deuteron analyzing power T_{20}, one notices here also that when $Q^2 > 0.4$ (GeV/c)^2, the beam-vector-deuteron analyzing power T_{11}^e starts to become model dependent. Comparing with the experimental data from MIT-Bates [7], also displayed in Fig. 3.6, one sees a general agreement.
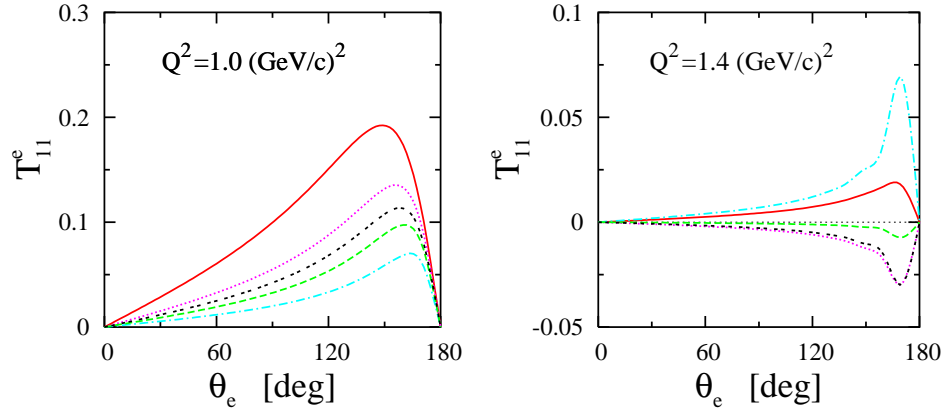
Figure 3.5: (Color online) The beam-vector-deuteron analyzing power T_{11}^e as a function of the electron scattering angle θ_e in the laboratory frame predicted at $Q^2 = 1.0$ (GeV/c)^2 (left panel) and 1.4 (GeV/c)^2 (right panel) with different NN potential models. Curve conventions are as in Fig. 3.2.
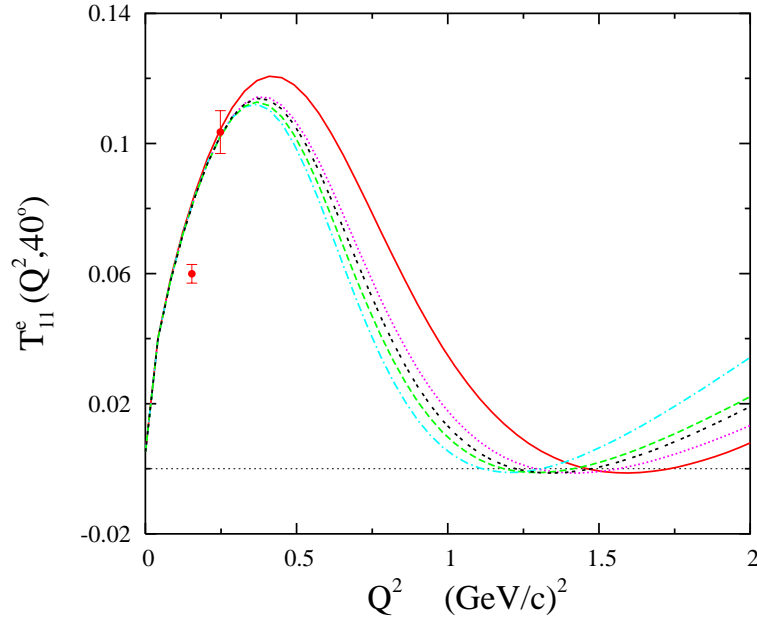

Figure 3.6: (Color online) The beam-vector-deuteron analyzing power T_{11}^e as a function of Q^2 predicted at $\theta_e = 40°$ with different NN potentials. Curve conventions are as in Fig. 3.2. Experimental data are from MIT-Bates [7].

4   Conclusion

Polarization obserables in elastic electron-deuteron scattering are predicted and compared with recent experimental data. Particular attention is paid to the tensor-deuteron

analyzing power T_{20} and the beam-vector-deuteron analyzing power T_{11}^e because of their importance in extracting the deuteron electromagnetic form factors which provide an intuitive picture of the internal deuteron structure. Furthermore, the sensitivity of the results to the deuteron wave function of different high-precision NN potentials is investigated. In the present work, we have used the Paris [24], Argonne $v18$ [25], one solitary boson-exchange OSBEP [27], Nijmegen-93 [26], and CD-Bonn [28] potential models. The results for analyzing powers were compared to each other and to experimental data. We found that the behaviors of the different NN potentials were nearly the same at low momentum transfers. In all cases the calculations agreed with one another and with the experimental data up to $Q^2 \simeq 0.5$ (GeV/c)^2, but slightly diverged at higher Q^2 because of the neglected contributions from the meson-exchange current and relativistic corrections [29]. The tensor-deuteron analyzing power T_{20} is found to be slightly dependent on the electron scattering angle up to $\theta_e \simeq 120°$, whereas the analyzing power T_{11}^e is found to be sensitive to θ_e.

We would like to point out that in addition to the tensor-deuteron analyzing power T_{20}, the beam-vector-deuteron analyzing power T_{11}^e can be used as an another tool for extracting the deuteron electromagnetic form factors. The magnetic dipole form factor G_M is strongly correlated with the vector polarization observable T_{11}^e. For this reason, one can use the BLAST data on the T_{11}^e asymmetry to extract the magnetic dipole form factor G_M.

Acknowledgements

References

[1] J. Carlson and R. Schiavilla, *Rev. Mod. Phys.* **70** (1998), 743.

[2] M. Garcon and W. Van orden, *Adv. Nucl. Phys.* **26** (2001), 293.

[3] R. Gilman and F. Gross, *J. Phys.* **G28** (2002), R37.

[4] J. Mandeville *et al.*, *Phys. Rev. Lett.* **72** (1994), 3325.

[5] J. S. Levinger, *Act. Phys.* **33** (1973), 135; T. J. Brady, E. L. Tomusiak, and J. S. Levinger, *Bull. Am. Phys. Soc.* **17** (1972), 438.

[6] M. J. Moravcsik and P. Ghosh, *Phys. Rev. Lett.* **32** (1974), 321.

[7] P. J. Karpius, PhD dissertation, University of New Hampshire, (2005).

[8] C. B. Crawford *et al.*, *Phys. Rev. Lett.* **98** (2007), 052301.

[9] D. Abbott *et al.*, *Eur. Phys. J.* **A7** (2000), 421.

[10] M. E. Schulze *et al.*, *Phys. Rev. Lett.* **52** (1984), 597.

[11] V. F. Dmitriev *et al.*, *Phys. Lett.* **B157** (1985), 143.

[12] R. A. Gilman *et al.*, *Phys. Rev. Lett.* **65** (1990), 1733.

[13] M. Garcon *et al.*, *Phys. Rev.* **C49** (1994), 2516.

[14] M. Ferro-Luzzi *et al.*, *Phys. Rev. Lett.* **77** (1996), 2630.

[15] M. Bouwhuis *et al.*, *Phys. Rev. Lett.* **82** (1999), 3755.

[16] D. Abbott *et al.*, *Phys. Rev. Lett.* **84** (2000), 5053.

[17] F. Gross, *Phys. Rev.* **142** (1966), 1025; F. Gross, *Phys. Rev.* **152** (1966), (E) 1517.

[18] T. W. Donnelly and A. S. Raskin, *Ann. Phys.* (N. Y.) **169** (1986), 247.

[19] A. R. Edmonds, *Angular Momentum in Quantum Mechanics*, Princeton University Press, 1968.

[20] S. E. Darden, in *Polarization Phenomena in Nuclear Physics*, edited by H. H. Barschall and W. Haeberli, The University of Wisconsin Press, Madison, Wisconsin, 1971.

[21] R. G. Arnold, C. E. Carlson, and F. Gross, *Phys. Rev.* **C23** (1981), 363.

[22] E. M. Darwish and M. Y. Hussein, *J. Kor. Phys. Soc.* **52** (2008), 226.

[23] M. I. Haftel, L. Mathelitsch, and H. F. K. Zingl, *Phys. Rev.* **C22** (1980), 1285.

[24] M. Lacombe, B. Loiseau, J. M. Richard, R. Vinh Mau, J. Côté, P. Pirès, and R. de Tourreil, *Phys. Rev.* **C21** (1980), 861.

[25] R. B. Wiringa, V. G. J. Stoks, and R. Schiavilla, *Phys. Rev.* **C51** (1995), 38.

[26] V. G. J. Stoks, R. A. M. Klomp, C. P. F. Terheggen, and J. J. de Swart, *Phys. Rev.* **C49** (1994), 2950.

[27] L. Jäde and H. V. von Geramb, *Phys. Rev.* **C55** (1997), 57; L. Jäde and H. V. von Geramb, *Phys. Rev.* **C57** (1998), 496; L. Jäde, *Phys. Rev.* **C58** (1998), 96.

[28] R. Machleidt, F. Sammarruca, and Y. Song, *Phys. Rev.* **C53** (1996), R1483; R. Machleidt, *Phys. Rev.* **C63** (2001), 024001.

[29] H. Arenhövel, F. Ritz and Th. Wilbois, *Phys. Rev.* **C61** (2000), 034002.